Sensing and Bio-Sensing Research 46 (2024) 100688

Contents lists available at ScienceDirect

Sensing and Bio-Sensing Research

journal homepage: www.elsevier.com/locate/sbsr

Analysis of plant physiological responses based on leaf color changes through the development and application of a wireless plant sensor

Kaori Kohzuma [a,c,d,*,1], Ko-ichiro Miyamoto [b,**]

[a] Graduate School of Life Sciences, Tohoku University, Sendai, Miyagi 980-8578, Japan
[b] Department of Electronic Engineering, Tohoku University, Sendai, Miyagi 980-8579, Japan
[c] Department of Biological Sciences, Graduate School of Science, The University of Tokyo, Tokyo 113-0033, Japan
[d] Astrobiology Centre, National Institutes of Natural Sciences, Mitaka 181-8588, Japan

ARTICLE INFO

Keywords:
Plant monitoring
Spectroscopic measurement
Leaf sensor
Remote sensing
Environmental response

ABSTRACT

Optical sensing has been used to monitor the physiological responses of plants noninvasively and in real-time. In this study, we developed a low-cost plant sensor that performed a spectroscopic measurement at eight wavelengths in the visible region. The sensor head of the system was attached directly to the underside of the leaf, not blocking the light, and eliminating correction work because of the constant distance between the sensor head and the sample. The collected data was shared in the cloud via a network, thereby enabling remote monitoring. The characteristics of the plant sensor as a spectral photometer were validated, with major wavelengths also showing good correlations with those of a conventional spectrometer. The reflectance of 620 nm in this sensor detected plant aging indicator chlorophyll, and 550 nm detected stress indicator xanthophyll. In the field test, these plant physiological responses, seasonal leaf color changes and environmental stresses, were observed remotely. The results indicate that the novel spectroscopic measurement from the underside of the leaf is effective to realize accurate and stable measurement of the plant leaf. The plant sensor can be a powerful tool in the field of agriculture and ecological study by realizing simultaneous, multi-point and remote monitoring at a low cost.

1. Introduction

Real-time monitoring of plant health is useful in ecological observation and agriculture. Plants, being sessile, must constantly respond to changing external conditions, such as light, temperature, and water [1–3]. Phenological day length and temperature changes significant influence plant aging [4,5]. Since the soil water content is not uniform, even when irrigated, plant-based monitoring is necessary [6,7]. Furthermore, information about the local weather and environment is particularly important in agriculture [8]. A high demand exists for spot observations of temperature, light intensity, humidity, and soil moisture, among many others [9–11]. Developing technology for monitoring environmental stresses noninvasively, remotely, and in real-time could collect information useful to various research fields.

As a modern response to these demands, “smart agriculture” and “precision agriculture,” which employ various sensors combined with the Internet of Things technologies, have swiftly developed to improve food profitability and economic profit. The data measured by sensors on local terminals is integrated via a network, enabling remote monitoring, which makes the technology highly suitable for agriculture [12,13]. Sensors that directly measure plants using the same strategy are called “wearable plant sensors”. Such technology for monitoring plants by attaching sensors to leaves or stalks has been reported [14 –18]. Accurate information about plants through direct sensing can help significantly in advancing smart agricultural technology.

In addition to physical information about plants, which most wearable plant sensors provide, numerous optical indices that reflect the biochemical state of plants can be utilized. For instance, photosynthetic pigments in plants that adjust chemically to changes in the external environment can be measured noninvasively using spectroscopy [19]. Soil Plant Analysis Development (SPAD) is widely used in agriculture as a useful index corresponding to chlorophyll levels [20]. It is calculated from differences between two transmission spectra, the 650 nm region, where chlorophyll absorbs the most of light, and the near-infrared

* Corresponding author at: Graduate School of Life Sciences, Tohoku University, Sendai, Miyagi 980-8578, Japan.
** Corresponding author. Department of Electronic Engineering, Tohoku University, Sendai, Miyagi 980-8579, Japan
E-mail addresses: kohzuma.kaori.7f@kyoto-u.ac.jp (K. Kohzuma), koichiro.miyamoto.d2@tohoku.ac.jp (K.-i. Miyamoto).
[1] Present address: Division of Applied Life Sciences, Graduate School of Agriculture, Kyoto University, Kyoto 606-8502, Japan.

https://doi.org/10.1016/j.sbsr.2024.100688
Received 21 May 2024; Received in revised form 30 August 2024; Accepted 16 September 2024
Available online 21 September 2024

region, where little absorption occurs. Although the SPAD device can perform measurements within a few seconds, measurements are made by inserting a leaf into the measuring head, which requires personnel to be on-site to use the device.

In contrast to on-site spectroscopic sensors, remote sensing using reflectance spectroscopy can assess multiple plants simultaneously from a distance. Several optical indices can be measured by reflectance spectroscopy to detect physiological changes in plants based on chemical changes in photosynthetic pigments. Normalized Difference Vegetation Index (NDVI) is the most common index of plant reflectance, a detection strategy similar to the SPAD [21]. The indicator normalizes the absorption region at 680 nm to the strongly reflective near-infrared region to determine whether a plant is green or not. NDVI contributes to the development of smart agriculture technologies, such as farm monitoring via satellite [22]. The photochemical Reflectance Index (PRI) detects xanthophyll pigments, which are measured at 530 nm and 570 nm [23]. Under environmental stresses such as excess light or drought, xanthophylls, such as violaxanthin (Vx), chemically change to zeaxanthin (Zx) [24 –26]. These changes are not visible, making the PRI an effective stress indicator [7,27].

Optical remote sensing is also widely used to monitor plants remotely and noninvasively using Unmanned Aerial vehicles (e.g., airplanes or drones). Although these are excellent tools, the sensor probe and target are far apart, and corrections must be made in response to the changing light environment [28,29]. In the remote sensing using a spectral camera, corrections are required for each test using a reflector, which makes management of the large data and analytical processing difficult. Therefore, a method that can easily and directly measure many plants simultaneously and allow instantaneous access to data could solve these problems.

In this study, we developed a stand-alone spectroscopic plant sensor that could perform remote, real-time plant health monitoring in the field, specifically changes in color, for over a month. The plant sensor detected changes in seasonal leaf colors and plant stress responses, measuring and collecting such data from the research site. The sensor head was attached directly to the underside of the leaf, which eliminated any correction work between sensor and target since the distance between the sensor head and sample remained constant. Another advantage is that changes in the same position can be observed. The collected data were shared to the cloud via a network. The plant sensor is demonstrated as a potentially valuable management tool in agricultural and environmental applications.

2. Material and methods

2.1. Measurement system

Our measurement system consists of a sensor head and controller connected by a flexible cable (Fig. 1A). The structure of the sensor head is shown in Fig. 1B. The sensor board (SEN0364, DFRobot, Shanghai, China) was enclosed with a cable connector board in an outer case. A multi-channel spectral sensor (AS7341, ams-OSRAM AG, Premstaetten, Austria) on the sensor board was used. In addition, two white LEDs (1SC3014W31A0WEL1, Xmbirghtek Optoelectronics Co., Ltd., Xiamen, China) also mounted on the sensor board were used as light sources in this study. The wavelength and the color temperature of the LEDs were about 400–800 nm and 5500–6500 K, respectively. It should be noted that the light source (LEDs) does not contain NIR light, thus the reflectance at NIR region cannot be obtained in this study. The luminous intensity of the LEDs was controlled by the spectral sensor at about 2.4 lm each. For outdoor measurements, an outer case was fabricated using a stereolithography 3D printer (Form3, Formlabs Inc., MA, USA). A homemade magnet holder and double-sided adhesive tape were used to attach the sensor head for short-term and long-term measurements, respectively.

Figure 1C shows the structure of the controller. A microcontroller (M5 stamp pico, M5Stack Technology Co., Ltd., Shenzhen, China) combined with a homemade shield board, lithium batteries (CR2, Panasonic Corp., Tokyo, Japan), and a voltage regulator (LXDC55, Murata Manufacturing Co., Ltd., Kyoto, Japan) were enclosed in an outer case. The outer case of the controller was fabricated using a fused deposition modelling 3D printer (L-Devo F300TP PLUS, Fusion Technology Co., Ltd., Tokyo, Japan). Both outer cases of the sensor head and controller were sealed with a silicone-based sealant for field use. The fabrication cost of the system was a few tens of dollars.

The measurement program used is developed in the Arduino Integrated Development Environment application (Arduino Software, Santa Fe, Argentina) and uploaded to the microcontroller. The microcontroller communicates with the sensor board to collect the spectroscopic data, which are then transferred to a cloud storage (Google Drive, Google LLC, CA, USA) via a Wi-Fi connection. The transferred data could be shared by users immediately.

2.2. Measurement principle

The concept of the measurement is shown in Fig. 2. The sensor head was attached to the abaxial side (underside) of a plant leaf (Fig. 2A), this is to avoid blocking light in the adaxial (upper side) The procedure of the measurement is as follows: (1) The LEDs in the sensor head were turned

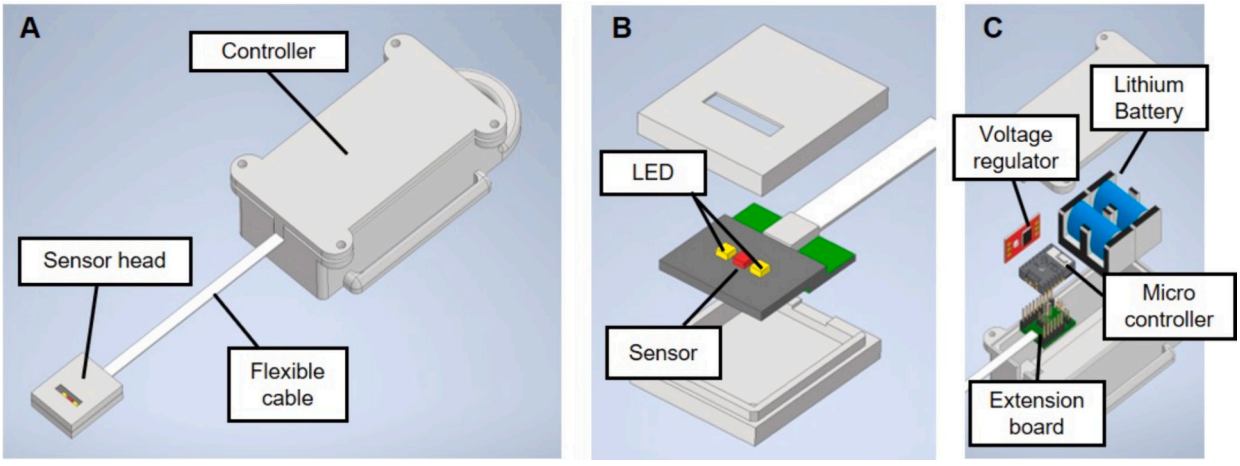

Fig. 1. (A) Illustration of the measurement system consisting of a sensor head and a controller unit. Configuration of (B) the sensor head and (C) the controller.

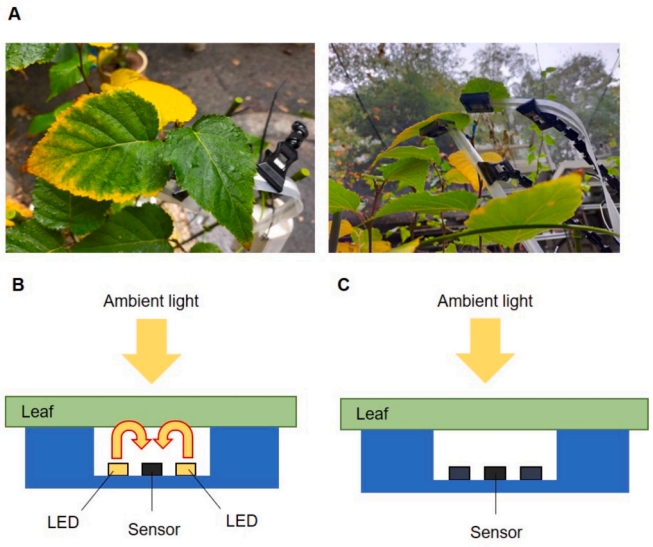

Fig. 2. Concept of the measurement. (A) The sensor head was attached to underside of the leaf. (B) Reflection from the underside of the leaf (LED turned on) and (C) ambient light (LED turned off) were measured. Under the light, the reflection spectrum of the leaf was obtained by subtracting LED-off from LED-on.

on, and a spectrum was recorded (Fig. 2B); (2) The LEDs were turned off, and a spectrum was measured to obtain background light through the leaf (Fig. 2C). The reflection spectrum of the leaf was obtained by subtracting measurement 2 from measurement 1. The reflection spectrum was then converted to reflectance using a reference spectrum of white standard. Here, nine channels of AS7341 were used, eight of which were used to collect the reflection spectrum at 410, 440, 470, 510, 550, 583, 620, and 670 nm. R_{410}, R_{440}, R_{470}, R_{510}, R_{550}, R_{583}, R_{620}, and R_{670} indicate the reflectance at each eight wavelengths, respectively. Note that these channels were tuned at each center wavelength by optical filters; thus, each channel has a broad sensitivity with full width at half maximum (FWHM) of tens of nanometers depending on the channel. Specifically, the FWHMs for channels at 410, 440, 470, 510, 550, 583, 620, and 670 nm are 29, 33, 36, 40, 42, 44, and 53 nm, respectively. The ninth channel was a broadband channel devoid of these filters to cover the entire range of the other eight channels. The broadband channel was used to estimate the intensity of ambient light through the leaf.

2.3. Plant materials

To collect spectral information by leaf color, approximately 90 variously colored leaves from 30 species were collected around the Hongo Campus of the University of Tokyo and at the Botanical Garden of the Ichimura Foundation in Atami City, Japan (Table 1, and Table S1). These leaves were measured immediately after picking. This experiment was conducted in the autumn season of 2022 to obtain leaves of various colors. *Arabidopsis thaliana* plants (accession Ws-02, and low ATP synthase mutant [30]) were grown in a growth chamber for 4–5 weeks under a 12-h light period (100 mmol photons m^2 s^{-1}) at 22 °C in Jiffy Mix (Sakata Seed Corporation, Japan).

2.4. Collection of library spectra

The library spectra were collected using two methods. The first reference spectrum was measured using a commercial spectrometer (FLAME-S-VIS-NIR-ES, Ocean Insight Inc., Orlando, FL, USA). The second reference spectrum was measured using the plant sensor. Both the spectrometer and sensor head were carefully attached to the sample to measure exactly the same position. The white LEDs mounted on the sensor board of the plant sensor were used as the light source.

Table 1
Plant species used in the analysis.

No.	Species
1	*Acer palmatum*
2	*Ardisia crenata*
3	*Ardisia japonica*
4	*Begonia Semperflorens*
5	*Betula ermanii*
6	*Camellia japonica*
7	*Camellia sinensis*
8	*Cerasus x yedoensis (Matsum.)*
9	*Coffea arabica*
10	*Cornus florida*
11	*Cornus kousa* subsp. *kousa*
12	*Dioscorea japonica*
13	*Diospyros kaki Thunb.*
14	*Enkianthus perulatus*
15	*Euonymus sieboldianus* var. *sieboldianus*
16	*Ginkgo biloba*
17	*Helianthus annuus*
18	*Hibiscus makinoi*
19	*Hydrangea macrophylla*
20	*Ilex pedunculosa*
21	*Liquidambar styraciflua*
22	*Malus domestica*
23	*Photinia* × *fraseri*
24	*Pieris japonica* subsp. *Japonica*
25	*Polygonum cymosum*
26	*Pseudocydonia sinensis*
27	*Rhododendron dilatatum*
28	*Rhodotypos scandens*
29	*Sarcandra glabra*
30	*Zelkova serrata*

2.5. Chlorophyll quantification

Leaf chlorophyll contents were measured using a SPAD instrument (SPAD-502 Plus, Konica Minolta, Japan). Furthermore, the chlorophyll content was assessed using the sensor unit by measuring reflectance at 620 nm (R_{620}). R_{620} was measured according to the procedure described above. The suitability of R_{620} as a wavelength for quantifying chlorophyll content was evaluated by correlating it with SPAD values.

2.6. Xanthophyll quantification and calculation of the de-epoxidation state

Xanthophylls, photosynthetic pigments, regulate light energy absorption through the xanthophyll cycle, converting Vx to Zx. Under stable conditions, Vx is predominant, but environmental stresses cause Vx to convert to Zx due to thylakoid lumen acidification [31]. To measure xanthophyll pigments, a leaf disk was ground in liquid nitrogen using a pestle and mortar and extracted with an equal volume of 82 % acetone. Samples were separated by high-performance liquid chromatography as described previously [7]. The de-epoxidation state (DEPS), which is the conversion rate of xanthophyll from Vx to Zx, was calculated using the following equation.

$$DEPS = (0.5 \times A) + Z/V + A + Z.$$

where V, A, and Z represent the violaxanthin, antheraxanthin, and zeaxanthin contents, respectively. An absorption coefficient in these xanthophylls was adjusted as previously described [32].

2.7. Long-term monitoring

Potted golden birch trees (Betula ermanii), approximately 1 m in height, were long-term monitored every two hours for two weeks in the experimental garden of the University of Tokyo (Bunkyo-ku, Tokyo). Sensor units were attached to green leaves before they turned color, and

the changes in leaf color to yellow or brown were tracked for approximately 2 weeks. The leaves of the plants were photographed with a camera every day. SPAD measurements were also performed. Spectroscopic measurements by the sensor were programmed every 2 h and automatically transferred to the cloud storage. The collected data were analyzed at Tohoku University (Sendai, Japan) using the stored data in the cloud storage.

3. Results and discussion

3.1. Validation of the plant sensor as a spectral photometer

To validate the capability of the plant sensor, the reflective spectra of gold birch measured by the plant sensor and spectrometer were compared. Fig. 3A and B show the upper side and underside leaves of gold birch, respectively, which are yellow in autumn. The reflective spectra were collected at four stages of color, from mature leaves to senescing and dying leaves: green, yellow-green, yellow, and brown. Since the pigment composition of the leaves is heterogeneous, leaf color varies widely depending on the position of a leaf. This is particularly evident during the fall foliage season when the components of photosynthetic pigments change drastically. Therefore, data were collected using both the plant sensor and spectrometer at the same leaf positions and the same spot on the underside of the leaves to compare the differences. In both measurements, the white LEDs were used as the light source.

In four-color leaves, the eight reflectance values collected by the plant sensor were compared with the continuous spectrum collected by the spectrometer in the visible region of 400–800 nm. Most of the eight values aligned with the continuous spectrum line, indicating that our

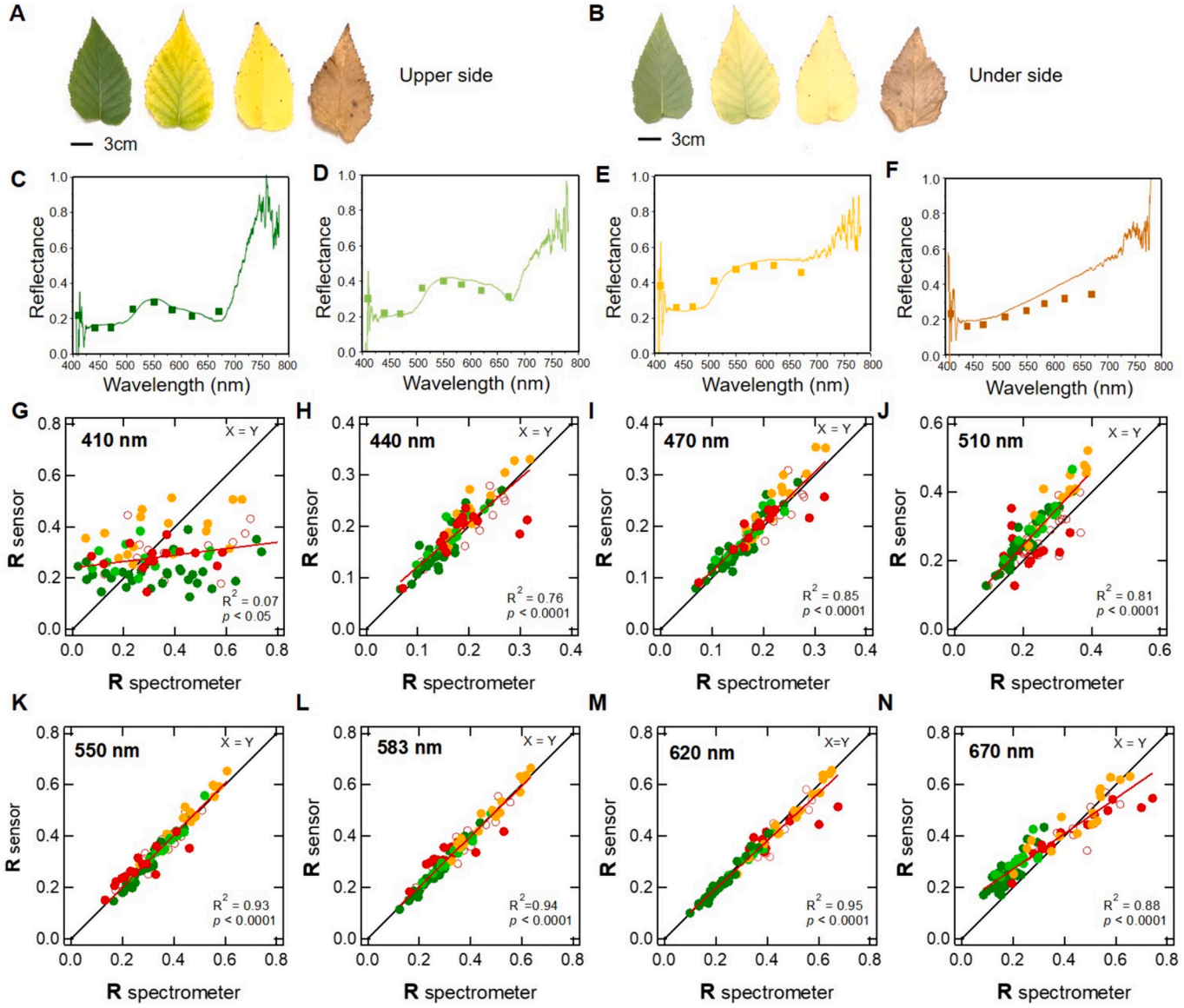

Fig. 3. Correlations of measurement using the plant sensor and a hyperspectral photometer at the same position on the leaf. (A–B) Images of the upper side and the underside of gold birch leaves in different stages, from maturity to senescence; scale bars = 3 cm. (C—F) Merged images of spectral data obtained from eight points by the plant sensor (410, 440, 470, 510, 550, 583, 620, and 670 nm), and a hyperspectral photometer from 400 to 800 nm. Four colors of lines and square points indicate the leaf colors evaluated (green, yellow-green, yellow, and red). These data were obtained at the same position on the underside of the leaf. (G–N) Correlation of the plant sensor (R sensor) and the hyperspectral data (R spectrometer) was plotted by wavelength. The same eight points measured by the plant sensor were extracted from the spectrometer data. Colored circles indicate leaf colors (green, yellow-green, yellow, and red). Red open circles indicate minor leaf colors such as brown or violet. The black lines indicate X = Y. (For interpretation of the references to color in this figure legend, the reader is referred to the web version of this article.)

plant sensor accurately reflected the expected reflectance. However, some discrepancies were observed with brown leaves, suggesting that in certain cases, additional calibration may be necessary for the accurate detection of dying leaves (Fig. 3C–3F). As photosynthetic pigments, such as chlorophyll, decompose in leaves during senescence, light absorption decreases, and reflectance intensity increases [33]. Expectedly, the reflectance was higher with yellow-green and yellow leaves than green ones (Fig. 3C–3E). Furthermore, as the leaf withered, and the water content of the leaf decreased, the reflectance decreased (Fig. 3F). Although signals that did not check were observed around the longer wavelengths at 600–700 nm in the withering brown leaf, the plant sensor detected most of the spectral features.

3.2. Reliability of the individual channels of the plant sensor

To verify the accuracy of the plant sensor, leaves of various colors were measured. Approximately 90 leaves from 30 plant species were examined (Table S1). The eight wavelengths corresponding to the channels of the plant sensor were extracted from the continuous spectra collected with the spectrometer and correlations were plotted by wavelength (Fig. 3G–1N). Red open circles indicate minor colors, such as orange, brown, and violet. The reflectance at 440, 470, 550, 583, and 620 nm were highly correlated (Fig. 3H–I and K–M). Slight deviations were observed in the reflectance at 510 and 670 nm (Fig. 3J and N). No correlation was observed in the reflectance at 410 nm (Fig. 3G). Common to the 410, 510, and 670 nm wavelengths is the weak intensity of the LED light source, especially at 410 nm. The nonuniformity in the light source at certain wavelengths reduced the sensor signal and the correlations. However, the reflectance at 510 and 670 nm can be easily corrected because they are regular, and the statistical difference is small, even though no complete match with X = Y was observed.

Extremely high correlations were observed at major wavelengths, indicating that the plant sensor can perform spectroscopic measurements of leaves at comparable sufficiency as the conventional spectrometer. In other words, the transition from green to yellow leaf color during senescence can be accurately detected. Conversely, if the color of the leaf sample was brown, the measurements tended to deviate from the X = Y line, even at highly correlated wavelengths.

3.3. Estimation of chlorophyll content

We estimated the chlorophyll content using the plant sensor. Chlorophyll is an essential molecule in plants that serves a light-harvesting function in photosynthetic reactions. Meanwhile, the amount of chlorophyll in plants is highly correlated with the amount of nitrogen, a protein component [34]. Therefore, measuring it indicates an estimate of plant health. SPAD is a well-known chlorophyll detector of the handy type [35]. The value is obtained as a difference in transmittance between the red (650 nm) wavelength, which chlorophyll absorbs, and near-infrared (940 nm) wavelength, which is not absorbed. Since the light source of this plant sensor has no near-infrared region, we considered using only the red region (620 nm or 670 nm), which shows the absorption of chlorophyll. As shown in Fig. 3C–F, the reflectance gradually increases from 620 nm to 650 nm during chlorophyll decomposition. Based on the results in Fig. 3, we decided to use 620 nm for estimating chlorophyll content due to its higher correlation coefficient (Fig. 3M and N).

We evaluated the correlation between reflectance at 620 nm (R_{620}) and SPAD values (Fig. 4). While a strong correlation was observed between SPAD and R_{620}, greater scatter was noted for yellow, red, and other minor colors as SPAD values decreased, where chlorophyll had completely degraded. This suggests that it may be necessary to consider the broader reflectance spectrum when assessing leaf color. Conversely, a better correlation was observed for yellow-green and green samples, indicating that R_{620} reflects chlorophyll content to some extent. Notably, changes in the chlorophyll degradation process were accurately

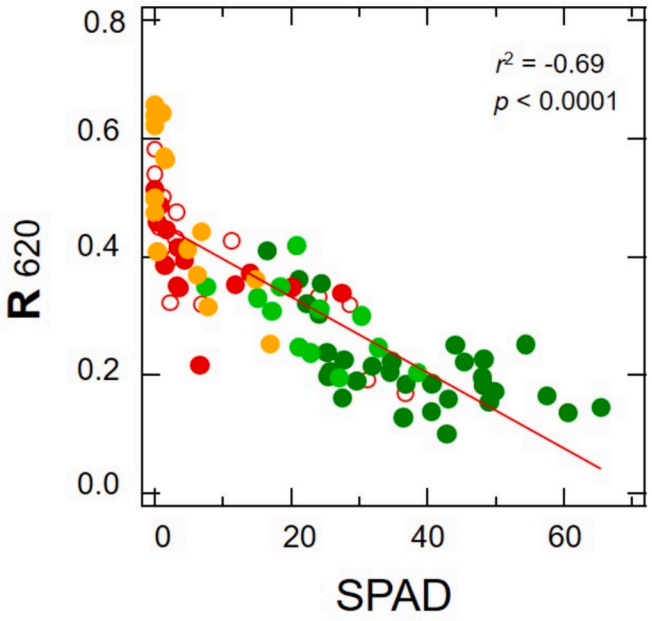

Fig. 4. Correlations between R_{620} and SPAD values. Colored circles indicate leaf colors (green, yellow-green, yellow, and red). Red open circles indicate minor leaf colors such as brown or violet. (For interpretation of the references to color in this figure legend, the reader is referred to the web version of this article.)

captured. These findings suggest that R_{620} can be used to monitor changes in chlorophyll content.

3.4. Monitoring of environmental stresses using chemical changes in photosynthesis pigments

Changes in reflectance can confirm chemical alterations in photosynthetic pigments. Xanthophylls regulate the amount of light energy absorbed through a chemical conversion from Vx to Zx (known as the xanthophyll cycle) [31]. During photosynthesis, when the absorption and consumption of light energy are in balance, the state remains as Vx. However, when this balance is disrupted by environmental stresses (e.g., excess light, drought, high temperature, or chilling), Vx is converted to Zx due to acidification of the thylakoid lumen. Zx has a reduced ability to transfer light energy to the photosystem, thereby preventing excessive light absorption and suppressing the generation of reactive oxygen in the chloroplast. When Vx is converted to Zx, the reflectance around 500–600 nm decreases [26]. Given that our sensor can measure at 550 nm, we investigated whether changes in xanthophylls could be detected.

We used an *Arabidopsis* mutant with a reduced amount of ATP synthase, which causes a high accumulation of Zx under growth light conditions [30], for analysis. ATP synthase synthesizes ATP using the energy of the proton gradient formed across the thylakoid membrane. Under low ATP synthase levels, the protons accumulated in the thylakoid lumen are not efficiently effluxed to the stroma, thereby acidifying the lumen. The lumen acidification activates the xanthophyll cycle; thus, Zx is highly accumulated in this mutant under light. In contrast, in the wild type, the conversion from Vx to Zx is not observed under growth light conditions. Sensors were attached to the underside of the leaf and performed measurements every 2 h in a growth chamber Fig. 5A shows the reflection patterns at the end of the night and day at the same position on the leaf. At around 550 nm, the reflectance in the mutant was downshifted compared with that in the wild type. Furthermore, the difference in the shift at 550 nm (ΔR_{550}) was more extensive in the mutant than in the wild type (Fig. 5B). The leaf disc was sampled at the end of the day and the end of the night, and the photosynthetic pigments

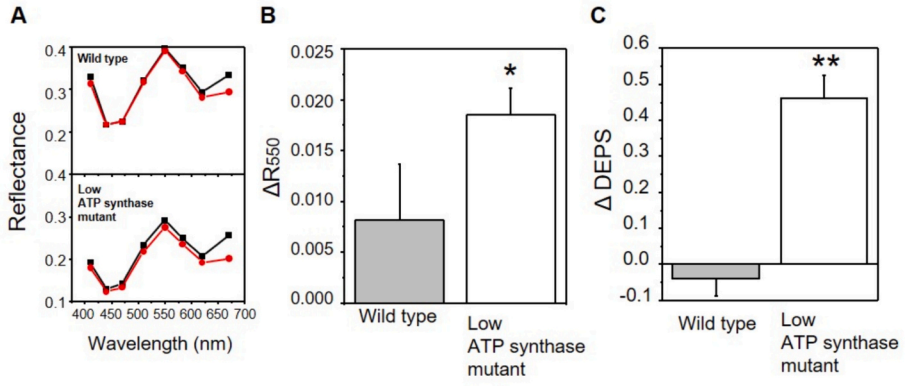

Fig. 5. Detection of xanthophyll pigment changes using R_{550} in Arabidopsis plants. (A) Reflectance changes under light and dark conditions in the wild type and low ATP synthase mutant with high zeaxanthin accumulation under growth light conditions. The black line indicates under dark conditions, and the red line indicates under light conditions. (B) Differences in R_{550} between dark and light conditions (ΔR_{550}) in the wild type (gray bar) and mutant (white bar). (C) Changes in xanthophyll changes (ΔDEPS) under dark and growth light conditions. Asterisks indicate significant differences compared with the wild type ($^{*}p < 0.05$, $^{**}p < 0.01$; Student's *t*-test). Data are expressed as mean ± standard deviation ($n = 3$). (For interpretation of the references to color in this figure legend, the reader is referred to the web version of this article.)

were quantified. DEPS, which is the conversion rate from Vx to Zx, was calculated. The difference in DEPS between the day and night (ΔDEPS) measurements was significantly larger in the mutant compared to the wild type (Fig. 5C).

The most appropriate wavelength to detecting xanthophyll cycles is reflectance at 530 nm (R_{530}), and PRI is known to normalize R_{530} by R_{570} [7]. Since the sensor does not perform measurements at 530 nm, we only used 550 nm and did not normalize. This is probably why the change in ΔR_{550} cannot completely reproduce the significant change in ΔDEPS. Given that this sensor can detect changes in xanthophylls even at 550 nm, it is expected to be effective for evaluating plant stress.

3.5. Remote observations of leaf phenology and environmental stresses

In the field, we monitored the color changes in Gold birch leaves for 2 weeks in the fall, and extracted and evaluated the changes in chlorophyll content and intensive light response based on the data. Fig. 6A shows the time course of reflectance at the eight wavelengths, with a black arrow indicating defoliation. The sensor head was fixed to the leaf; thus, the collection of data did not stop even after the leaf fell.

One advantage of this sensor is its capability to automatically repeat data collection at the same position on the leaf, thereby eliminating the need for normalization techniques such as NDVI or PRI. Additionally, the sensor can provide approximate estimates of local sunlight intensities. Fig. 6B presents the time course of the signal from the sensor's broadband channel, reflecting relative solar illumination. The sunlight piercing through the leaf was detected as ambient light (see Fig. 2C). It is possibly affected by the leaf color. However, the signal of the broadband channel is an integration of the wide wavelength and color changes that occurred over a week; thus we assumed that the plot of Fig. 6B reflects the intensities of local sunlight. Fig. 6C shows images captured during the measurement.

The leaf color changed from green to yellow on Day 7, then dark yellow, and then brown at the end of the measurement period. Reflectance increased as the green color increased, which indicates a decrease in chlorophyll content (Fig. 6A). As the pigment faded and the leaf withered, the reflectance decreased. The spectrum patterns at each stage matched the catalog data for typical leaf colors (Fig. 6D and Fig. 3C–3F). As seen on Days 1–3, the spectrum with a broad peak at 500 nm is the typical reflectance pattern of a green leaf, whereas the spectrum with enhanced reflectance at 600 nm corresponds to a yellow color. The spectrum obtained on Day 13 of a dead leaf showed an overall decrease in reflectance. A relative increase in reflectance was observed from 583 to 670 nm, which is characteristic of dead leaves.

Based on these, the correlation between R_{620} and SPAD value shown in Fig. 4, the amount of chlorophylls of Gold birch was also estimated by the reflectance at 620 nm. A high correlation was observed between the change in reflectance at 620 nm and the actual SPAD value (Fig. 6E). These results demonstrate that estimating changes in chlorophyll contents in real-time is possible through remote observation. However, the data after defoliation was removed in Fig. 6E because SPAD is unable to measure accurate values in browned and dead leaves. The spectral pattern in detecting chlorophyll using R_{620} should also be confirmed.

In addition, we verified whether the photosynthesis response could be monitored based on changes in R_{550}. The changes in R_{550} with the light conditions (with dark as 0) were plotted against the ambient light intensities (Fig. 6F). A significant correlation was observed between the amount of sunlight and R_{550} in leaves that maintained their green color until day 6. Furthermore, the amplitude of the ΔR_{550} under intense light was large. By contrast, no correlation was observed between R_{550} and the amount of sunlight for leaves that turned yellow after day 7. These results demonstrated that monitoring the response to light in leaves that retained sufficient pigment is possible based on changes in R_{550}, whereas photosynthetic reactions could not be tracked in yellowed leaves.

3.6. Sensor scalability and future challenges

The plant sensor detected responses to long-term phenological aging and transient defense responses to intense light by detecting photosynthetic pigments such as chlorophylls and xanthophylls. However, the current measurements could not evaluate the photosynthetic ability of plants. To determine the exact photosynthetic rate, the functionality of chlorophyll fluorescence analysis must be implemented. Since chlorophyll fluorescence can be detected from signals within 680–780 nm [36], our plant sensors may be modified to do the evaluation.

As a fast physiological change, it is known that chloroplasts move in the cell to avoid excess light [37]. In this study, we observed relatively slow responses occurring over several hours to days; thus, the chloroplast movement was not a concern. When measuring short-term responses, chlorophyll movement and the detection of photosynthetic responses on the underside of the leaf should be considered.

The sensor head was directly attached to the underside of the leaf using double-stick tape. Contact between the leaf and a gas-permeable polyester film using a silicone-based adhesive did not damage the leaf during long-term measurements and did not affect the plant's responses. However, the chamber between the leaf and sensor head is a semi-enclosed space. A relationship exists between wind speed on the leaf surface and the rate of photosynthesis [38]. The measurement of

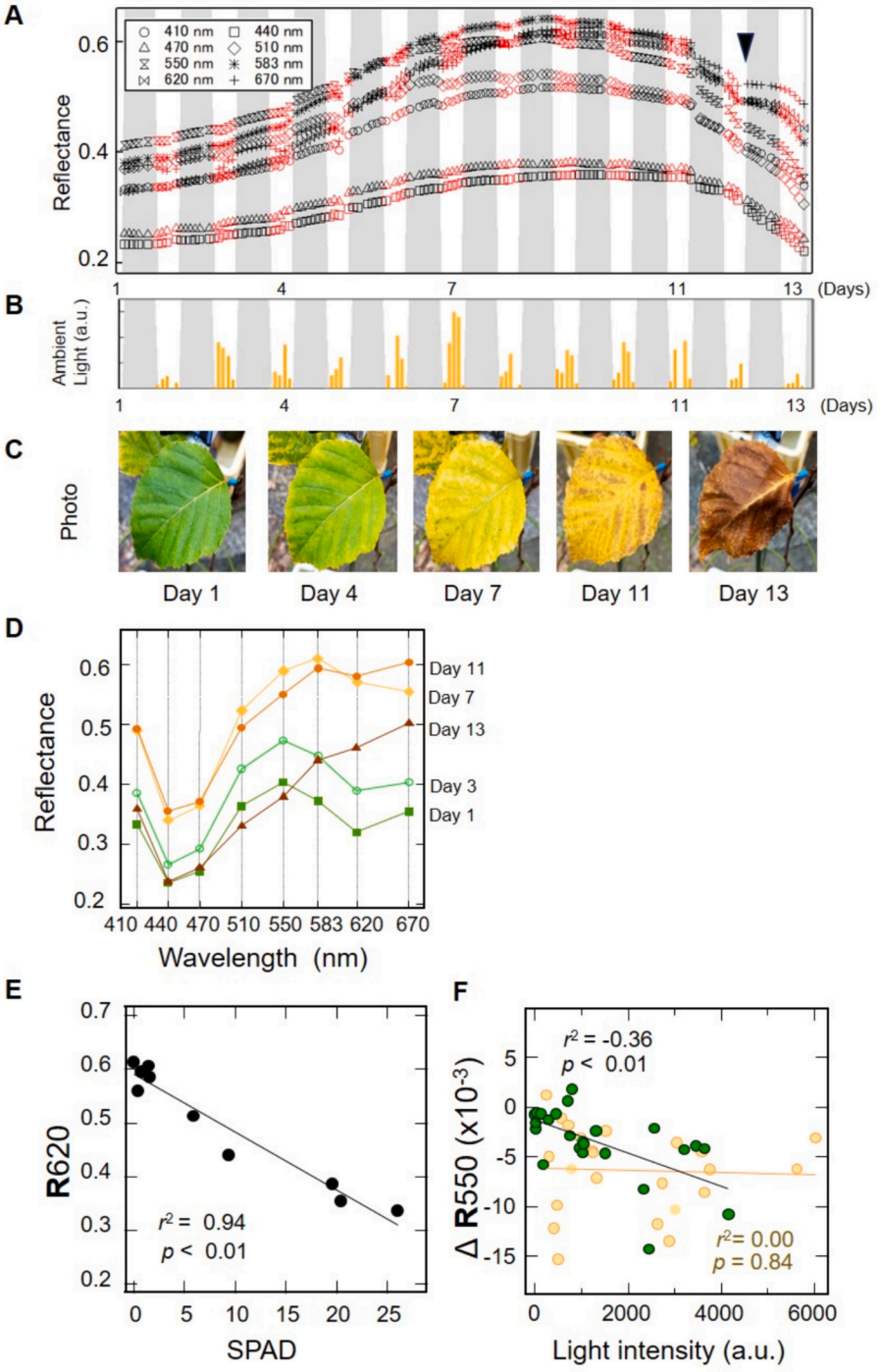

Fig. 6. Remote observations of leaf color changes in gold birch in the field. (A) The observation was performed for 13 days in December 2022. The gray and white background indicates night and day. The black arrow indicates the point of defoliation. (B) Ambient light intensity. The relative intensity was detected by the broadband channel. (C) Images of leaf color changes. (D) Reflectance patterns from Days 1–13. The line colors indicate the actual leaf colors evaluated. (E) Correlations between R_{620} and Soil Plant Analysis Development (SPAD) before the defoliation. Data for R_{620} was measured at the same point as the SPAD measurements. (F) Correlations between ΔR_{550} and relative light intensities. Green circles indicate data until Day 6 when leaves were still green. Light yellow circles indicate data after Day 7, at which point leaves turned from yellow to brown. (For interpretation of the references to color in this figure legend, the reader is referred to the web version of this article.)

photosynthetic processes, such as gas exchange, must be verified for accuracy if performed.

In Fig. 3, reflectance patterns of 90 colored leaves were obtained. These data enabled the assessment of wavelength detection capabilities of the plant sensor, but also provided a catalog for evaluating the relationship between color and reflectance patterns. PCA analysis or machine learning utilizing these data would enable the prediction of leaf color based on the newly acquired patterns.

In this study, we demonstrated that the plant sensor holds significant potential for various applications. For further advancement in field applications, it is essential to carefully consider both the advantages and limitations of the plant sensor. Table S2 presents a comparison with a

conventional spectrometer, highlighting that the plant sensor offers benefits in terms of cost, size, and Wi-Fi connection. However, the fixed wavelength and limited resolution represent notable drawbacks. In addition to the technical specifications of the plant sensor, improving the usability of the sensor system from a practical standpoint is also critical.

4. Conclusions

In this study, we described the development of a small and low-cost spectral sensor, which could be directly attached to the underside of the leaf, for detecting real-time physiological changes in plants in response to environmental changes. The sensor facilitated data collection by enabling connectivity to the cloud via Wi-Fi encased in a waterproof package containing a battery. The colors and light responses of plants were monitored in real-time using the information obtained through a sensor at a remote experimental field. The plant sensor can collect information at eight wavelengths in the visible region that is comparable to that of the commercial spectrometer. This paper demonstrates that changes in chlorophyll content and plant stress responses can be detected with high precision at 620 nm (R_{620}) and through the difference between dark and light measurements at 550 nm (ΔR_{550}). The ability to detect changes in xanthophylls at 550 nm also suggests that this sensor can effectively evaluate plant stress. Additionally, the sensor offers the advantage of automatic collection of data at the same position on the leaf, thereby eliminating the need for normalization techniques such as NDVI or PRI. Moreover, it can provide rough estimates of local sunlight intensities. We obtained catalog data from the colors of 90 leaf samples. The catalog data could be used as training data in predicting leaf color remotely. The plant sensor can be a powerful tool for agricultural and ecological observation.

Supplementary data to this article can be found online at https://doi.org/10.1016/j.sbsr.2024.100688.

CRediT authorship contribution statement

Kaori Kohzuma: Writing – review & editing, Writing – original draft, Visualization, Validation, Supervision, Software, Resources, Project administration, Methodology, Investigation, Funding acquisition, Formal analysis, Data curation, Conceptualization. **Ko-ichiro Miyamoto:** Writing – review & editing, Writing – original draft, Visualization, Validation, Supervision, Software, Resources, Project administration, Methodology, Investigation, Funding acquisition, Formal analysis, Data curation, Conceptualization.

Declaration of competing interest

The authors declare the following financial interests/personal relationships which may be considered as potential competing interests:

Kaori Kohzuma reports financial support was provided by Japan Science and Technology Agency. Ko-ichiro MIYAMOTO reports financial support was provided by Japan Society for the Promotion of Science. Ko-ichiro MIYAMOTO reports financial support was provided by Ichimura Foundation for New Technology. Ko-ichiro MIYAMOTO reports financial support was provided by Tsukuba Innovation Arena. If there are other authors, they declare that they have no known competing financial interests or personal relationships that could have appeared to influence the work reported in this paper.

Data availability

The data that has been used is confidential.

Acknowledgments

We thank Tatsuo Yoshinobu (Tohoku University), Kouki Hikosaka (Tohoku University), Ichiro Terashima (The university of Tokyo), Haruhiko Taneda (The university of Tokyo), Kenji Takizawa (AstroBiology center), Kentaro Ifuku (Kyoto University), David Kramer (Michigan State University) for assistance with provide research environments and stimulating discussions. This work was supported by JST FORESTO Program (Grant Number MJFR2276, Japan), JSPS KAKENHI (Grant Number JP22K19196), Ichimura Foundation for new technology, and TIA collaborative research program.

References

[1] Q. Wang, Y. Wu, W. Wu, L. Lyu, W. Li, A review of changes at the phenotypic, physiological, biochemical, and molecular levels of plants due to high temperatures, Planta 259 (2024) 57, https://doi.org/10.1007/s00425-023-04320-y.
[2] Y. Wang, J. Wang, R. Sarwar, W. Zhang, R. Geng, K. Zhu, X. Tan, Research progress on the physiological response and molecular mechanism of cold response in plants, Front. Plant Sci. 15 (2024) 1334913, https://doi.org/10.3389/fpls.2024.1334913.
[3] K. Kohzuma, J.A. Cruz, K. Akashi, S. Hoshiyasu, Y.N. Munekage, A. Yokota, D. M. Kramer, The long-term responses of the photosynthetic proton circuit to drought, Plant Cell Environ. 32 (2009) 209–219, https://doi.org/10.1111/j.1365-3040.2008.01912.x.
[4] N. Budianti, M. Naramoto, A. Iio, Drone-sensed and sap flux-derived leaf phenology in a cool temperate deciduous forest: a tree-level comparison of 17 species, Remote Sens. 14 (2022) 2505, https://doi.org/10.3390/rs14102505.
[5] P.P. Dion, J. Brisson, B. Fontaine, L. Lapointe, Light acclimation strategies change from summer green to spring ephemeral as wild-leek plants age, Am. J. Bot. 103 (2016) 963–970, https://doi.org/10.3732/ajb.1500503.
[6] S.O. Ihuoma, C.A. Madramootoo, Sensitivity of spectral vegetation indices for monitoring water stress in tomato plants, Comput. Electron. Agric. 163 (2019) 104860, https://doi.org/10.1016/j.compag.2019.104860.
[7] K. Kohzuma, M. Tamaki, K. Hikosaka, Corrected photochemical reflectance index (PRI) is an effective tool for detecting environmental stresses in agricultural crops under light conditions, J. Plant Res. 134 (2021) 683–694, https://doi.org/10.1007/s10265-021-01316-1.
[8] T.G. Doeswijk, K.J. Keesman, Improving Local Weather Forecasts for Agricultural Applications, Proceedings of the Second IASTED International Multi-Conference on Automation, Control, and Information Technology - Signal and Image Processing, 2005, pp. 107–112. https://edepot.wur.nl/35773.
[9] T.T. Rajapaksha, A. Alexander, L. Fernando, A. Than, L.H. Nguyen, Real-time weather monitoring and IoT-based palmtop device for smart agriculture, SN Comput. Sci. 3 (2022) 91, https://doi.org/10.1007/s42979-021-00961-6.
[10] K.R. Gsangaya, S.S.H. Hajjaj, M.T.H. Sultan, L.S. Hua, Portable, wireless, and effective internet of things-based sensors for precision agriculture, international journal of Int, J. Environ. Sci. Technol. 17 (2020) 3901–3916, https://doi.org/10.1007/s13762-020-02737-6.
[11] J. Jin, Y. Wang, H. Jiang, X. Chen, Evaluation of microclimatic detection by a wireless sensor network in forest ecosystems, Sci. Rep. 8 (2018) 16433, https://doi.org/10.1038/s41598-018-34832-7.
[12] D. Thakur, Y. Kumar, A. Kumar, P.K. Singh, Applicability of wireless sensor networks in precision agriculture: a review, Wirel. Pers. Commun. 107 (2019) 471–512, https://doi.org/10.1007/s11277-019-06285-2.
[13] A. Bhujel, J.K. Basak, F. Khan, E. Arulmozhi, M. Jaihuni, T. Sihalath, D. Lee, J. Park, H.T. Kim, Sensor systems for greenhouse microclimate monitoring and control: a review, J. Biosyst. Eng. 45 (2020) 341–361, https://doi.org/10.1007/s42853-020-00075-6.
[14] J.A. Barbosa, V.M.S. Freitas, L.H.B. Vidotto, G.R. Schleder, R.A.G. de Oliveira, J. F. da Rocha, L.T. Kubota, L.C.S. Vieira, H.C.N. Tolentino, I.T. Neckel, A.L. Gobbi, M. Santhiago, R.S. Lima, Biocompatible wearable electrodes on leaves toward the on-site monitoring of water loss from plants, ACS Appl. Mater. Interfaces 14 (2022) 22989–23001, https://doi.org/10.1021/acsami.2c02943.
[15] B. Peng, X. Wu, C. Zhang, C. Zhang, L. Lan, J. Ping, Y. Ying, In-time detection of plant water status change by self-adhesive, water-proof, and gas-permeable electrodes, ACS Appl. Mater. Interfaces 15 (2023) 19199–19208, https://doi.org/10.1021/acsami.3c01789.
[16] H. Ibrahim, S. Moru, P. Schnable, L. Dong, Wearable plant sensor for in situ monitoring of volatile organic compound emissions from crops, ACS Sens. 7 (2022) 2293–2302, https://doi.org/10.1021/acssensors.2c00834.
[17] N.I. Hossain, S. Tabassum, A hybrid multifunctional physicochemical sensor suite for continuous monitoring of crop health, Sci. Rep. 13 (2023) 9848, https://doi.org/10.1038/s41598-023-37041-z.
[18] C. Zhang, C. Zhang, X. Wu, J. Ping, Y. Ying, An integrated and robust plant pulse monitoring system based on biomimetic wearable sensor, npj Flexible Electron. 6 (2022) 43, https://doi.org/10.1038/s41528-022-00177-5.
[19] E. Bihar, E.J. Strand, C.A. Crichton, M.N. Renny, I. Bonter, T. Tran, M. Atreya, A. Gestos, J. Haseloff, R.R. McLeod, G.L. Whiting, Self-healable stretchable printed electronic cryogels for in-vivo plant monitoring, npj Flexible Electron. 7 (2023) 48, https://doi.org/10.1038/s41528-023-00280-1.
[20] M.S. Kubar, C. Wang, R.S. Noor, M. Feng, W. Yang, K.A. Kubar, K. Soomro, C. Yang, H. Sun, H. Mohamed, W.F.A. Mosa, Nitrogen fertilizer application rates and ratios promote the biochemical and physiological attributes of winter wheat, Front. Plant Sci. 13 (2022) 1011515, https://doi.org/10.3389/fpls.2022.1011515.

[21] Y. Peng, A. Nguy-Robertson, T. Arkebauer, A.A. Gitelson, Assessment of canopy chlorophyll content retrieval in maize and soybean: implications of hysteresis on the development of generic algorithms, Remote Sens. 9 (2017) 226, https://doi.org/10.3390/rs9030226.
[22] S. Yang, S. Li, B. Zhang, R. Yu, C. Li, J. Hu, S. Liu, E. Cheng, Z. Lou, D. Peng, Accurate estimation of fractional vegetation cover for winter wheat by integrated unmanned aerial systems and satellite images, front, Plant Sci. (2023) 1220137, https://doi.org/10.3389/fpls.2023.1220137.
[23] J.A. Gamon, C.B. Field, W. Bilger, O. Bjorkman, A.L. Fredeen, J. Penuelas, Remote sensing of the xanthophyll cycle and chlorophyll fluorescence in sunflower leaves and canopies, Oecologia 85 (1990) 1–7, https://doi.org/10.1007/BF00317336.
[24] J. Peñuelas, I. Filella, J.A. Gamon, Assessment of photosynthetic radiation-use efficiency with spectral reflectance, New Phytol. 131 (1995) 291–296, https://doi.org/10.1111/j.1469-8137.1995.tb03064.x.
[25] J.A. Gamon, L. Serrano, J.S. Surfus, The photochemical refectance index: an optical indicator of photosynthetic radiation use efficiency across species, functional types, and nutrient levels, Oecologia 112 (1997) 492–501, https://doi.org/10.1007/s004420050337.
[26] K. Kohzuma, K. Hikosaka, Physiological validation of photochemical reflectance index (PRI) as a photosynthetic parameter using Arabidopsis thaliana mutant, Biochem. Biochem. Biophys. Res. Commun. 498 (2018) 52–57, https://doi.org/10.1016/j.bbrc.2018.02.192.
[27] L. Yudina, E. Sukhova, E. Gromova, V. Nerush, V. Vodeneev, V. Sukhov, A light-induced decrease in the photochemical reflectance index (PRI) can be used to estimate the energy-dependent component of non-photochemical quenching under heat stress and soil drought in pea, wheat, and pumpkin, Photosynth. Res. 146 (2020) 175–187, https://doi.org/10.1007/s11120-020-00718-x.
[28] P. Sishodia, R.L. Ray, S.K. Singh, Applications of remote sensing in precision agriculture: a review, Remote Sens. 12 (2020) 3136, https://doi.org/10.3390/rs12193136.
[29] S.F.D. Gennaro, P. Toscano, M. Gatti, S. Poni, A. Berton, A. Matese, Spectral comparison of UAV-based hyper and multispectral cameras for precision viticulture, Remote Sens. 14 (2022) 449, https://doi.org/10.3390/rs14030449.
[30] K. Kohzuma, C. Dal Bosco, A. Kanazawa, A. Dhingra, W. Nitschke, J. Meurer, D. M. Kramer, Thioredoxin-insensitive plastid ATP synthase that performs moonlighting functions, Proc. Natl. Acad. Sci. USA 109 (2012) 3293–3298, https://doi.org/10.1073/pnas.111572810.
[31] B. Demmig-Adams, W.W. Adams, Photoprotection and other responses of plants to high light stress, Annu. Rev. Plant Physiol. Plant Mol. Biol. 43 (1992) 599–626, https://doi.org/10.1146/annurev.pp.43.060192.003123.
[32] S.S. Thayer, O. Björkman, Leaf xanthophyll content and composition in sun and shade determined by HPLC, Photosynth. Res. 23 (1990) 331–343, https://doi.org/10.1007/BF00034864.
[33] Y. Zhang, C. Wang, J. Huang, F. Wang, R. Huang, H. Lin, F. Chen, K. Wu, Exploring the optical properties of leaf photosynthetic and photo-protective pigments in vivo based on the separation of spectral overlapping, Remote Sens. 12 (2020) 3615, https://doi.org/10.3390/rs12213615.
[34] R.F. Muñoz-Huerta, R.G. Guevara-Gonzalez, L.M. Contreras-Medina, I. Torres-Pacheco, J. Prado-Olivarez, R.V. Ocampo-Velazquez, A review of methods for sensing the nitrogen status in plants: advantages, disadvantages and recent advances, Sensors (Basel). 13 (2013) 10823–10843, https://doi.org/10.3390/s130810823.
[35] Z. Yuan, Q. Cao, K. Zhang, S.T. Ata-Ul-Karim, Y. Tian, Y. Zhu, W. Cao, X. Liu, Optimal leaf positions for SPAD meter measurement in Rice, front, Plant Sci. 7 (2016) 719, https://doi.org/10.3389/fpls.2016.00719.
[36] L.E.G. Brissette, C.Y.S. Wong, D.P. McHugh, J. Au, E.L. Orcutt, M.C. Klein, T. S. Magney, Tracking canopy chlorophyll fluorescence with a low-cost light emitting diode platform, AoB Plants 15 (2023) plad069, https://doi.org/10.1093/aobpla/plad069.
[37] M. Wada, Chloroplast movement, Plant Sci. 210 (2013) 177–182, https://doi.org/10.1016/j.plantsci.2013.05.016.
[38] J.M. Costa, O.M. Grant, M.M. Chaves, Thermography to explore plant-environment interactions, J. Exp. Bot. 64 (2013) 3937–3949, https://doi.org/10.1093/jxb/ert029.